



30. Numerical simulation of $SU(2)_c$ high density state

Shin Muroya ¹⁾, Atsushi Nakamura ²⁾ and Chiho Nonaka ³⁾

¹⁾ *Tokuyama Women's Coll. Shunan, 745-8511, Japan*

²⁾ *RIISE, Hiroshima Univ., Higashi-Hiroshima 739-8521, Japan*

³⁾ *Dept. of Phys., Duke Univ., Durham, NC27708-0305, USA*

Abstract

We report a study of the high baryon number density system with use of the two-color lattice QCD with Wilson fermions[1]. First we investigate thermodynamical quantities such as the Polyakov line, gluon energy density, and baryon number density in the (κ, μ) plane, where κ and μ are the hopping parameter and chemical potential, respectively. Then we calculate propagators of meson ($\bar{q}\Gamma q$) and baryon ($q\Gamma q$) states in addition to the potential between quark lines.

1 Introduction

Phase structure of the strongly interacting matter is the hottest topics of the recent hadron physics[2]. In addition to the well known confinement-deconfinement phase transition in high temperature, QCD may have a much richer structure in high density. Experimentally, a wide region of the (T, μ) plane has been investigated by AGS, SPS and RHIC, and a higher density region is left as an important task of GSI and JPARC.

Lattice QCD is expected to provide nonperturbative information of QCD as the first principle calculation. However, numerical study of lattice QCD with chemical potential is extremely difficult, because at finite μ the fermion determinant $\det D$ becomes complex, which appears in the Euclidean path integral measure,

$$Z = \int \mathcal{D}U \mathcal{D}\bar{\psi} \mathcal{D}\psi e^{-\beta S_G - \bar{\psi} D \psi} = \int \mathcal{D}U \det D e^{-\beta S_G}. \quad (1)$$

Though there exist several remarkable progresses in the lattice calculations with the finite chemical potential[3], it is still quite difficult to study the regions around critical μ at low temperature by lattice QCD simulations. In order to circumvent the above difficulty, in the present paper, two-color QCD has been investigated [1].

2 Actions and algorithm

We introduce the chemical potential in the conventional manner,

$$D(x, x') = \delta_{x, x'} - \kappa \sum_{i=1}^3 \left\{ (1 - \gamma_i) U_i(x) \delta_{x', x+i} + (1 + \gamma_i) U_i^\dagger(x') \delta_{x', x-i} \right\} - \kappa \left\{ e^{+\mu} (1 - \gamma_4) U_4(x) \delta_{x', x+4} + e^{-\mu} (1 + \gamma_4) U_4^\dagger(x') \delta_{x', x-4} \right\}. \quad (2)$$

For the gauge action, we employ the plaquette and Iwasaki improved actions. Here, we report the improved action case only. Little is known about dynamical fermion simulations in which the chemical potential is introduced, therefore, we employ an algorithm where the ratio of the determinant,

$$\frac{\det D(U + \Delta U)}{\det D(U)} = \det(I + D(U)^{-1} \Delta D) \quad (3)$$

is evaluated explicitly in each Metropolis update process, $U \rightarrow U + \Delta U$, where $\Delta D \equiv D(U + \Delta U) - D(U)$. This algorithm has a long Markov step and is very reliable. Numerical costs are, however, huge and we are restricted to small lattices. In the following studies, therefore, we check that the results obtained are not sensitive to the boundary conditions.

3 Study of the (κ, μ) Parameter Space

Since there are few color $SU(2)$ lattice studies using Wilson fermions with finite μ , we first investigate the relevant parameter space. We measure the Polyakov line, $\langle L \rangle$ on a 4^4 lattice by changing β for $\mu = 0$ and $\kappa = 0.150$ and choose the region where $\langle L \rangle$ is small, i.e., the system is in the confinement phase at zero baryon number density. We set $\beta = 0.7$ on the basis of this analysis.

At this value of β , we measure $\langle L \rangle$, its susceptibility, $\frac{\partial \langle L \rangle}{\partial \mu}$, the gluon energy density, $\langle E_g \rangle = \langle \frac{1}{V_s} \frac{\partial}{\partial (1/T)} S_G \rangle$ and the number density, $\langle n \rangle = \frac{T}{V_s} \frac{\partial}{\partial \mu} \log Z$, as a function of μ and κ . Here S_G is the gauge action and $V_s = N_x N_y N_z$ is the spatial volume of the lattice. In Fig.1, we show $\langle L \rangle$, $\langle n \rangle$ and $\langle E_g \rangle$ on a 4^4 lattice as a function of μ and κ . They increase as μ becomes large and show the deconfinement behavior. We observe that the simulation always breaks down when we increase μ further.

In Fig.2, we show the Polyakov line susceptibilities $\kappa = 0.150$ and 0.175 under the antiperiodic spatial boundary condition and for $\kappa = 0.160$ under the periodic boundary condition. All exhibit a peak when μ increases, which indicates a deconfinement transition. All quantities support the picture that at large μ the system undergoes the transition from the confinement to the deconfinement phase. In addition to the increase of $\langle L \rangle$ and $\langle E_g \rangle$, the rapid increase of $\langle n \rangle$ is observed. The

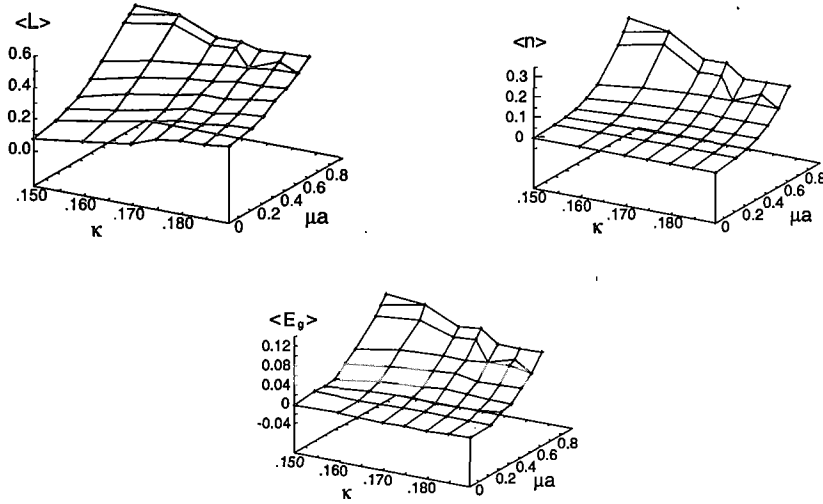


Figure 1: The Polyakov line $\langle L \rangle$, the number density $\langle n \rangle$ and the gluon energy $\langle E_g \rangle$ as a function of κ and μ . Lattice size is 4^4 .

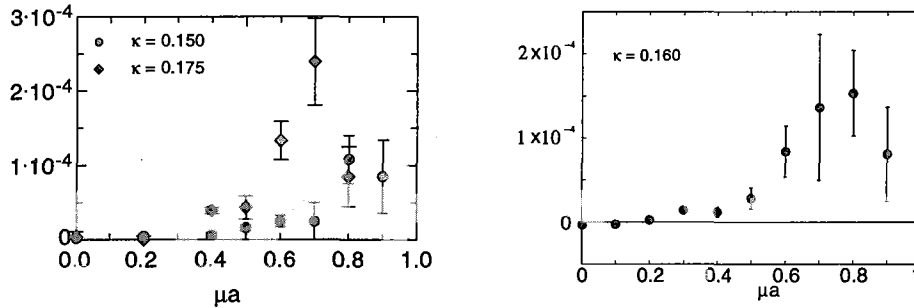


Figure 2: Polyakov line susceptibility, $\partial\langle L \rangle / \partial\mu = \langle (L - \langle L \rangle)(n - \langle n \rangle) \rangle$, as a function of μ on $4^3 \times 8$ lattice. (a) $\kappa = 0.150, 0.175$ under the anti-periodic spatial boundary condition and (b) $\kappa = 0.160$ under the periodic boundary condition.

instability at large μ may be an indication of a new phase with the diquark condensation. Although the behavior of all quantities supports the existence of the deconfinement phase at large μ , there are some indications that suggest a more complicated phase. In many cases, we observe a second peak in the Polyakov line susceptibility at large μ .

4 Hadron propagators

We calculate correlations of color singlet hadron operators, $M(x) = \bar{\psi}_\alpha^a(x)\Gamma_{\alpha\beta}\psi_\beta^a(x)$ and $B(x) = \epsilon^{ab}\psi_\alpha^a(x)(C\Gamma)_{\alpha\beta}\hat{\tau}\psi_\beta^b(x)$, where Γ is the product of Dirac matrices and $\hat{\tau}$ is a Pauli matrix acting on flavor indices. C is the charge conjugation matrix and a and b are color indices. We set $\hat{\tau} = \tau_2$ or $\tau_2\vec{\tau}$ so that the wave function is totally

antisymmetric.

To our knowledge, no study of the behaviors of hadrons including vector mesons at finite baryon density has been performed using lattice QCD. Vector mesons are important since they provide information at several stages of heavy ion collision in the form of lepton pairs.

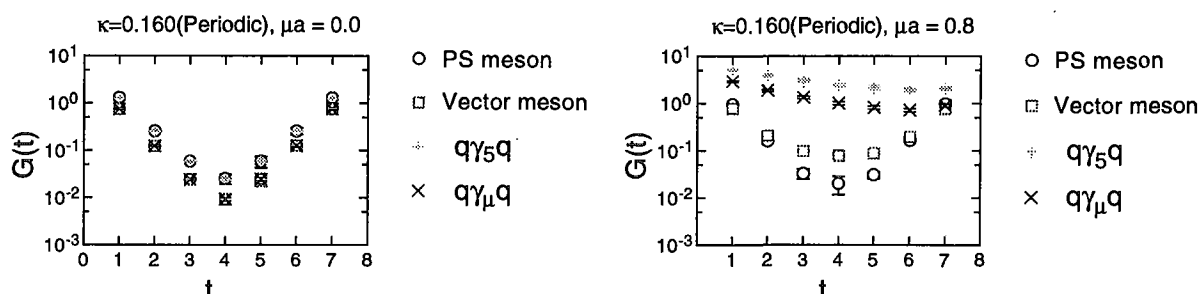


Figure 3: Hadron propagators at $\mu a = 0$ (left) and $\mu a = 0.8$.

In Fig.3, we show propagators of the pseudoscalar and vector mesons and those of the scalar ($\Gamma = \gamma_5$) and pseudovector (γ_ν) baryons for $\mu = 0$ and $\mu a = 0.8$, where a is the lattice spacing. The most prominent feature here is that the vector meson propagator is strongly modified at $\mu a = 0.8$. Its slope is more gradual than that for the pseudoscalar, i.e., the vector meson becomes lighter.

If the sudden drop of the vector meson mass is not a special feature of the color SU(2) model, this may be the first lattice QCD result to show the reduction of the vector meson mass in the medium.

5 $qq, \bar{q}q$ potential at finite density

Here we focus on the behavior of $qq, \bar{q}q$ potential in order to understand the vacuum structure at high chemical potential numerically. In this calculation the lattice size is $8 \times 4 \times 12 \times 4$ and the number of flavor is 3.

From Polyakov line correlations, color average heavy quark potential is calculated as,

$$e^{-V_0(\vec{R})/T} = \frac{C}{N_c} \langle \text{Tr}L(\vec{R}) \frac{1}{N_c} \text{Tr}L(0) \rangle \quad (4)$$

where $C = 1/(\frac{1}{N_c} \langle \text{Tr}L(0) \rangle)^2$. However there is no difference between $qq, \bar{q}q$ color average potential in color SU(2). One can also obtain color dependent potential, i.e. singlet (V_1) and triplet potential (V_3) for $q\bar{q}$ system: $N_c \times \bar{N}_c = 1 \oplus (N_c^2 - 1)$,

$$e^{-V_1(\vec{R})/T} = \frac{C}{N_c} \langle \text{Tr}L(\vec{R})L^\dagger(0) \rangle, \quad (5)$$

$$e^{-V_3(\vec{R})/T} = C \frac{N_c^2}{N_c^2 - 1} \langle \frac{1}{N_c} \text{Tr}L(\vec{R}) \frac{1}{N_c} L^\dagger(0) \rangle. \quad (6)$$

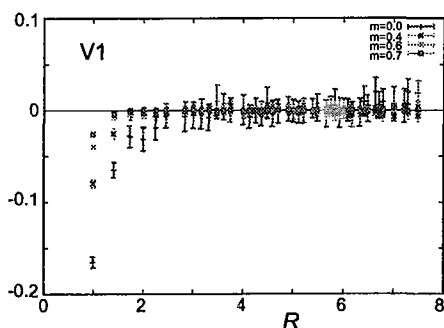


Figure 4: Color singlet potential V_1 for $\mu = 0.0, 0.4, 0.6$ and 0.7 .

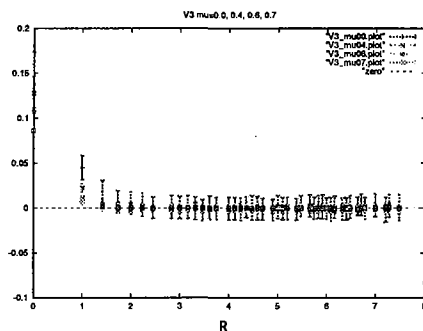


Figure 5: Color triplet potential V_3 for $\mu = 0.0, 0.4, 0.6$ and 0.7 .

For qq system color symmetric (V_s) and anti-symmetric (V_a) potential can be also evaluated: $N_c \times N_c = \frac{1}{2}N_c(N_c + 1) \oplus \frac{1}{2}N_c(N_c - 1)$,

$$e^{-V_s(\vec{R})/T} = \frac{N_c}{N_c+1} \frac{\langle \frac{1}{N_c} \text{Tr}L(\vec{R}) \frac{1}{N_c} \text{Tr}L(0) \rangle}{(\frac{1}{N_c} \langle \text{Tr}L(0) \rangle)^2} + \frac{1}{N_c+1} \frac{\langle \frac{1}{N_c} \text{Tr}L(\vec{R})L(0) \rangle}{(\frac{1}{N_c} \langle \text{Tr}L(0) \rangle)^2}, \quad (7)$$

$$e^{-V_a(\vec{R})/T} = \frac{N_c}{N_c-1} \frac{\langle \frac{1}{N_c} \text{Tr}L(\vec{R}) \frac{1}{N_c} \text{Tr}L(0) \rangle}{(\frac{1}{N_c} \langle \text{Tr}L(0) \rangle)^2} - \frac{1}{N_c-1} \frac{\langle \frac{1}{N_c} \text{Tr}L(\vec{R})L(0) \rangle}{(\frac{1}{N_c} \langle \text{Tr}L(0) \rangle)^2}. \quad (8)$$

In color $SU(2)$, $V_1 = V_a$ and $V_3 = V_s$ even at $\mu \neq 0$. Therefore if there would be difference between qq and $q\bar{q}$ states, it is due to some Dirac structure.

In Figs.4 and 5, we plot the (preliminary) results of color singlet potential and color triplet potential, respectively. We can see that the rotational invariance is good due to the renormalization group improved gauge action. The singlet (triplet) potential is attractive (repulsive) force and the forces between $qq/\bar{q}q$ become weaker as μ increases. Medium effect appears in these forces and this behavior suggests the confinement-deconfinement phase transition. Here we fix the gauge in Lorenz gauge for the color-dependent force and gluon propagators discussed in the following.

6 Concluding remarks

In this study, we have investigated energy density of gluon sector, number density, Polyakov line and its susceptibility together with potential between quark lines in (κ, μ) parameter space.

We observed a sudden reduction of the vector meson mass when the chemical potential was increased.

Our lattice here is small, but results for the case of periodic and antiperiodic boundary conditions in the spatial directions show the same qualitative behavior. The behavior of the thermodynamic quantities together with that of the Polyakov line supports the standard picture, i.e., QCD undergoes a transition from the confinement to the deconfinement phase. We have observed several indications in the

susceptibility and gluon propagators, which may suggest a more complicated phase at finite baryon number density.

Acknowledgment

We would like to thank T. Kunihiro, T. Inagaki and T. Schäfer for helpful discussions. This work is supported by Grant-in-Aide for Scientific Research by Monbu-Kagaku-sho (No.11440080, No. 12554008 and No. 13135216), and ERI, Tokuyama Univ.. Simulations were performed on SR8000 at IMC, Hiroshima M Univ., SX5 at RCNP, Osaka Univ., SR8000 at KEK.

References

- [1] Shin Muroya, Atsushi Nakamura and Chiho Nonaka, hep-lat/02011010, Phys. Lett. B551 (305-310)(2003).
- [2] for example, see the proceedings of the YITP-RCNP Workshop “Chiral Restoration in Nuclear Medium”, held at Kyoto, Japan, October 7-9, 2002; the proceedings of “XVI International Conference on Particles and Nuclei ” held at Osaka, Japan, September 30 - October 4, 2002.
- [3] S. Choe et al., Phys. Rev. D63 (2001) 054501; Z. Fodor and S. D. Katz, JHEP 0203 (2002) 014; Phys. Lett. B534 (2002) 87; C. R. Allton et al., hep-lat/0204010; Ph. deForcrand and O. Philipsen, hep-lat/0205016; M. D’Elia and M-L. Lombardo, hep-lat/0205022.